

Low-complexity improved schemes for ACO-OFDM based on hartley transform or real-fourier transform over AWGN channel

Max Fréjus Owolabi SANYA ^{1,*}, Hermine IGABOUY CHOBLI ¹, Stanislas Arthur Oladélé SANYA ², Zola Cédric Bosco ALONOUMI ¹, Dounicia Laurence AGLIKPO ¹ and Fifamè Merci-Ange MAGNIDET ³

¹ Department of Computer Science and Telecommunications, GIT/ EPAC-University of Abomey-Calavi, Abomey-Calavi, Atlantique, Benin.

² Department of Applied Mathematical and Engineering Science Laboratory (LISMA), UNSTIM University, Abomey, Benin

³ Ecole Doctorale Sciences De l'Ingénieur (ED-SDI), University of Abomey-Calavi, Abomey-Calavi, Atlantique, Benin.

World Journal of Advanced Research and Reviews, 2025, 25(02), 1085-1098

Publication history: Received on 20 December 2024; revised on 31 January 2025; accepted on 04 February 2025

Article DOI: <https://doi.org/10.30574/wjarr.2025.25.2.0506>

Abstract

As a widely used Intensity Modulation and Direct Detection (IM/DD) system, Asymmetrically Clipped Optical Orthogonal Frequency Division Multiplexing (ACO-OFDM) is considered one of the most promising modulation techniques for high-speed optical communications. Conventional ACO-OFDM uses Hermitian Symmetry (HS) to guarantee a real signal, which results in high computational complexity. The Real Discrete Fourier Transform (RDFT) and Discrete Hartley Transform (DHT) offer alternative approaches to generating real-valued OFDM signals without the need for HS. In the existing literature, various modified techniques have been proposed to enhance ACO-OFDM in terms of bit error rate (BER) or spectral efficiency. However, these methods often suffer from high computational complexity or poor BER performance due to DC offsets and low-frequency noise. To the best of our knowledge, few studies have explored low-complexity yet improved ACO-OFDM schemes that use alternatives to the conventional Discrete Fourier Transform (DFT). In this context, this paper investigates the implementation of Diversity-Combining (DC) and Improved Noise Cancellation (INC) techniques using the Discrete Hartley Transform (DHT) and Real-DFT in an ACO-OFDM scheme over an Additive White Gaussian Noise (AWGN) channel. Simulations conducted in MATLAB 2021 show that both DHT-based and Real-DFT ACO-OFDM achieve similar BER performance compared to conventional ACO-OFDM. Furthermore, the proposed schemes demonstrate a 3 dB power gain in an AWGN channel over traditional ACO-OFDM. Given their low complexity and high performance, DHT-based and Real-DFT INC-ACO-OFDM emerge as promising candidates for optical network systems. Among them, DHT-based solutions are particularly advantageous due to their lower computational complexity.

Keywords: ACO-OFDM; AWGN; Bit Error Rate; Discrete Hartley Transform; Improved Noise Cancellation method

1. Introduction

Over the years, researchers have explored different techniques to enhance the capacity of optical communication networks, driven by the exponential growth of services like high-speed internet, cloud computing, and the Internet of Things. Traditionally, the most common modulation format used in these systems is Non-Return-to-Zero On-Off Keying (NRZ-OOK) [1]-[3], a simple technique that encodes one bit per symbol by switching an optical LED source on and off. Although NRZ-OOK is easy to implement and offers good energy efficiency at low data rates, it suffers from high sensitivity to noise and interference. To address this, researchers have turned to alternative methods such as Pulse Position Modulation (PPM) [4]-[5] and Pulse Amplitude Modulation (PAM) [6]. These methods improve the energy efficiency and throughput compared with NRZ-OOK. However, they remain vulnerable to inter-symbol interference (ISI)

* Corresponding author: Max Fréjus Owolabi SANYA,

due to multipath distortion [7]. To overcome these limitations, Orthogonal Frequency Division Multiplexing (OFDM) has emerged as a key solution for high-speed optical systems. It uses the Fast Fourier Transform (FFT) to convert data into multiple subcarriers and its Inverse (IFFT) to get the data back. By applying FFT, the signal is split into orthogonal frequency components, optimizing spectrum utilization and significantly mitigates ISI [7], enabling higher transmission rates [8]. The FFT and IFFT process are accelerated and made cost-effective by the availability of numerous FFT and IFFT algorithms, as well as advancements in field-programmable gate arrays (FPGA) [9]. Despite the advantages of OFDM systems, they face several challenges, including a high peak-to-average power ratio (PAPR), which necessitates radiofrequency amplifiers to operate over a wide linear range [10]. Also, OFDM is very sensitive to frequency offsets and channel variations, which can lead to ISI and Inter-Carrier Interference (ICI). To mitigate these issues, precise synchronization between transceivers is essential.

Many studies have investigated techniques to address these issues and improve the OFDM performances. Significant attention has been given to replacing or combining the FFT block in conventional OFDM systems with alternative orthogonal transforms, such as the Discrete Cosine Transform (DCT), Discrete Sine Transform (DST), Walsh-Hadamard Transform (WHT), Wavelet Packet Transform (WPT), and DHT block [11]. The primary objectives of these approaches are to enhance system performance—such as reducing PAPR or bit error rates (BER)—or to decrease computational complexity [12]-[17].

Conventional OFDM cannot be directly applied to optical systems that use Intensity Modulation with Direct Detection (IM/DD) because these systems require a real and positive signal. To remedy this, Hermitian Symmetry must be applied before performing the IDFT. The DHT, in particular, is notable [13] for its real-valued nature, requiring only real arithmetic operations. This makes it especially suitable for real-valued signals, such as those used in optical communication systems [14]. Furthermore, the DHT and its inverse (IDHT) share an identical kernel, allowing for the use of the same circuitry in both the transmitter and receiver [16]. Alternative approaches for obtaining a real-valued signal without relying on Hermitian symmetry are introduced in [18]-[19]. The first technique, presented in [19], uses a half-size IFFT/FFT, offering low implementation complexity by transmitting both the real and next, the imaginary parts of the complex signal. The second method, known as Real-Discrete Fourier Transform (Real-DFT) in [20], uses the standard IFFT/FFT size but processes only the real part of the signal after zero-padding half of the IFFT inputs [21]. We find the Real-DFT and DHT approaches particularly interesting due to their low computational complexity, making them viable alternatives to the traditional FFT/IFFT in OFDM systems. For this reason, they have been included in this paper.

To generate non-negative signals, the initial solution was DCO-OFDM (DC-biased Optical OFDM) which converted the bipolar OFDM signal into a positive unipolar signal by introducing a direct current (DC) bias. But, the high DC bias resulted in reduced power efficiency. To improve power efficiency, Asymmetrically Clipped Optical OFDM (ACO-OFDM) was proposed [19], [21]. However, enhancing the BER or spectral efficiency of ACO-OFDM in optical communications remains a challenge [22]-[25]. ACO-OFDM is shown for example, to have the same data rate as FLIP-OFDM and U-OFDM [23], [24]. Asymmetrically clipped DC-biased optical ADO-OFDM is the first hybrid technique that combines aspects of both DCO and ACO-OFDM [22]. While ADO-OFDM maintains the same data rate as DCO-OFDM, it demonstrates poor BER performance compared to the previous mentioned methods [23]-[27]. The asymmetrically and symmetrically clipped optical ASCO-OFDM technique [26] is another hybrid approach that achieves a higher data rate than ACO-OFDM and FLIP-OFDM, while keeping a comparable BER performance to DCO-OFDM. Superimposed OFDM schemes have emerged to increase power efficiency, such as Hybrid ACO-OFDM (HACO-OFDM) [27] and Layered ACO-OFDM (LACO-OFDM) [28]. Their spectral and power efficiency is higher than that of ACO-OFDM. However, their transmitter consists of multiple OFDM modulation blocks superimposed together, and the receiver requires an iterative OFDM demodulation to detect the superimposed components. This results in significant higher computational complexity for the entire system. For low-complexity, advanced non-hybrid techniques like Diversity-Combined ACO-OFDM (DC-ACO-OFDM) [11]-[12] and our proposed Improved Noise Cancellation ACO-OFDM (INC-ACO-OFDM) [16] have been implemented using DHT or Real-DFT, rather than the conventional DFT.

This paper extends our work [16] about Improved Noise Cancellation DHT-based ACO-OFDM to alternative low-complexity scheme. To the best of our knowledge, Improved Noise Cancellation technique or Diversity-Combining demodulation for Real-DFT approach has never been explored. We propose a low-complexity ACO-OFDM scheme which implements Real-DFT along with Diversity-Combining or the Improved Noise Cancellation method, aiming to achieve high power efficiency over an AWGN channel. The performance of the system is studied and compared in terms of BER and computational complexity.

The rest of this paper is organized as follows. Section 2 describes the proposed ACO-OFDM schemes and methodology used. Section 3 presents the simulation results and gives some related discussion. Finally, the conclusion is presented in Section 4.

2. Material and methods

In this section, we begin by outlining the principles of the conventional ACO-OFDM scheme and its variants using Real-DFT and DHT transforms. Following that, we present detailed descriptions of the DC-ACO-OFDM and INC-ACO-OFDM architectures based DHT and Real-DFT, along with a comparison to the corresponding existing methods. After that, we provide a comprehensive overview of the methodology used.

2.1. Conventional ACO-OFDM technique

The block diagram of conventional ACO-OFDM scheme is depicted in Figure 1. In ACO-OFDM, data symbols are constrained to exhibit Hermitian Symmetry as in (1) and are transmitted exclusively on odd subcarriers, while the even subcarriers remain unused and set to zero [27]-[28].

$$X_k = X_{2N-k}^*, \quad 0 < k < N \dots\dots\dots (1)$$

The input vector $X = [0, X_0, 0, X_1, 0, \dots, 0, X_{2N-1}]$ with an IFFT input size of $2N$, must satisfy condition (1). As a result, the corresponding time-domain signal x is real and exhibits anti-symmetry, as shown by equation (2). However, in intensity-modulated direct detection (IM/DD) optical systems, a signal cannot be transmitted directly, because the light intensity is always non-negative [18].

$$x_k = -x_{k+N}, \quad 0 < k < N \dots\dots\dots (2)$$

To address this issue, zero clipping is applied after the cyclic prefix (CP) is added, allowing negative values to be suppressed without any loss of information. At the receiver, the CP is removed and data symbols are recovered from the odd subcarriers after FFT operation, channel estimation and equalization.

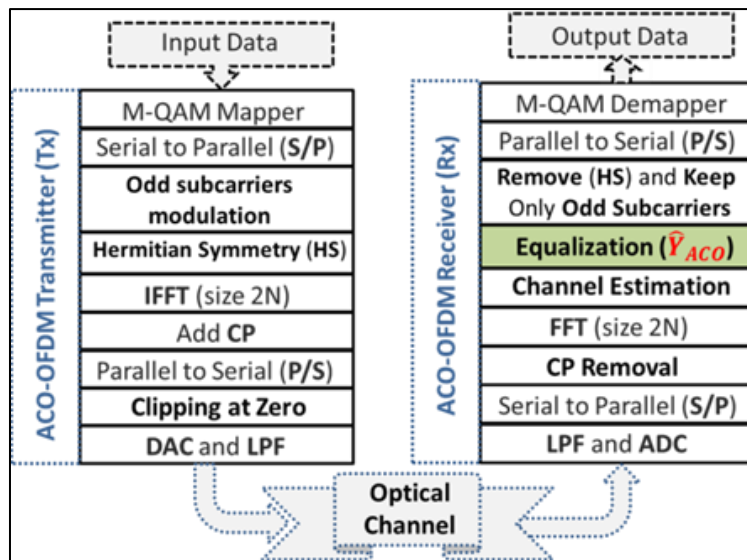


Figure 1 Conventional ACO-OFDM block diagram

2.2. DHT-based ACO-OFDM scheme

Since the Hartley transform only operates on real numbers, it is preferable to use modulations based on real values, such as binary phase shift keying (BPSK) and multi-level pulse amplitude modulation (M-PAM). As with DFT-based ACO-OFDM, in DHT ACO-OFDM, the information is also transmitted on odd-numbered subcarriers only [16]-[17]. As shown in Figure 2, since the signal obtained after the IDHT block is bipolar, so it is clipped at zero to ensure it is real and positive. At the receiver, the reverse process of the transmitter is performed to accurately reconstruct the signal. According to [13],[14] the DHT symbol is given by (3), where N is the IDHT/DHT size, $k = 0, 1, 2, \dots, N-1$, and $x(n)$ the n th symbol sequence.

$$h(k) = \frac{1}{\sqrt{N}} \sum_{n=0}^{N-1} x(n) \left[\cos\left(\frac{2\pi kn}{N}\right) + \sin\left(\frac{2\pi kn}{N}\right) \right] \dots\dots\dots (3)$$

Similarly, to return to the frequency domain, a DHT transform is applied as described by (4):

$$x(n) = \frac{1}{\sqrt{N}} \sum_{k=0}^{N-1} h(k) \left[\cos\left(\frac{2\pi kn}{N}\right) + \sin\left(\frac{2\pi kn}{N}\right) \right] \dots\dots\dots(4)$$

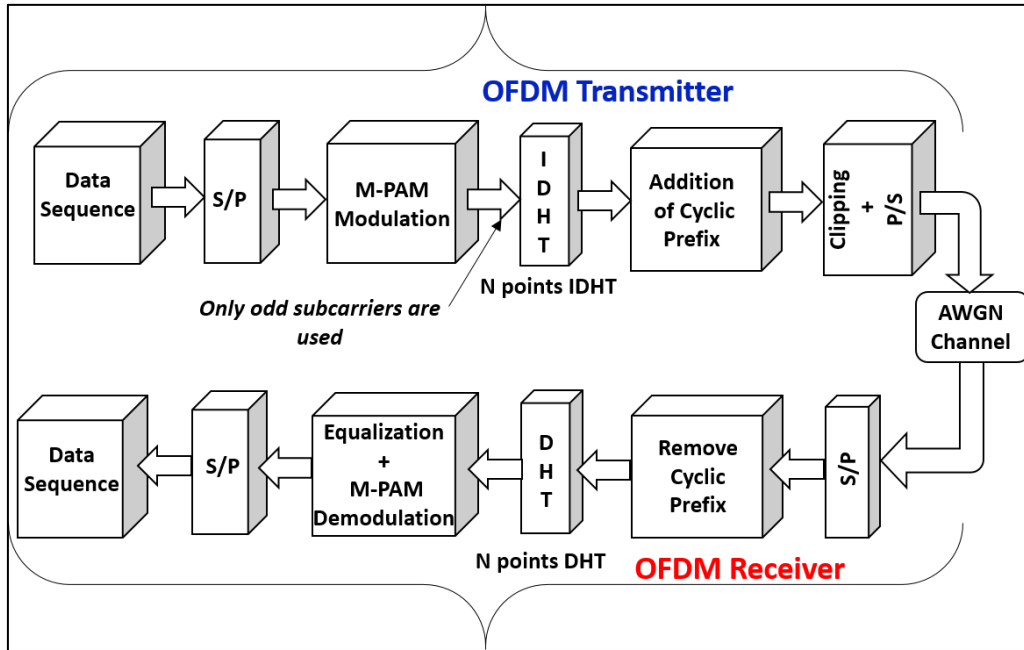


Figure 2 Block diagram of DHT-based ACO-OFDM scheme

2.3. Real-DFT-based ACO-OFDM scheme

The key idea behind the Real-DFT algorithm is to replace the complex conjugates of the subcarriers with zeros, which maintains the symmetry of the data for periodic signals [20]. In optical communication systems, Real-DFT is typically used for signal processing to recover the original complex signal from its real-valued representation. The Real-DFT technique is particularly useful when dealing with systems where the signal is real-valued, as it allows for the extraction of complex modulation symbols using only the real part of the signal. As shown in Figure 3-a, the mapped subcarriers $X(n)$ are zero-padded before the IFFT, rather than applying Hermitian Symmetry as in (5). In the case of Real-DFT-based ACO-OFDM, only the odd subcarriers are used for data transmission. Therefore, its IFFT input symbol vector \tilde{X} must satisfy equation (6).

$$\tilde{X}(n) = \begin{cases} 0 & \text{for } n = 0, \\ X(n-1) & \text{for } n \in \{1, 2, \dots, N\}, \dots\dots\dots(5) \\ 0 & n \in \{N+1, \dots, 2N-1\}. \end{cases}$$

$$\tilde{X} = \left[0, X_0, 0, X_1, \dots, 0, X_{\frac{N}{2}-1}, \underbrace{0, \dots, 0}_{N \text{ zeros}} \right] \dots\dots\dots(6)$$

At the output of the IFFT block, after the CP is added, only the real component $x_R(n')$ of size $N' = 2N+N_{CP}$ is used. This is then clipped to zero to $x_{RDFT-ACO}(n')$ before transmission.

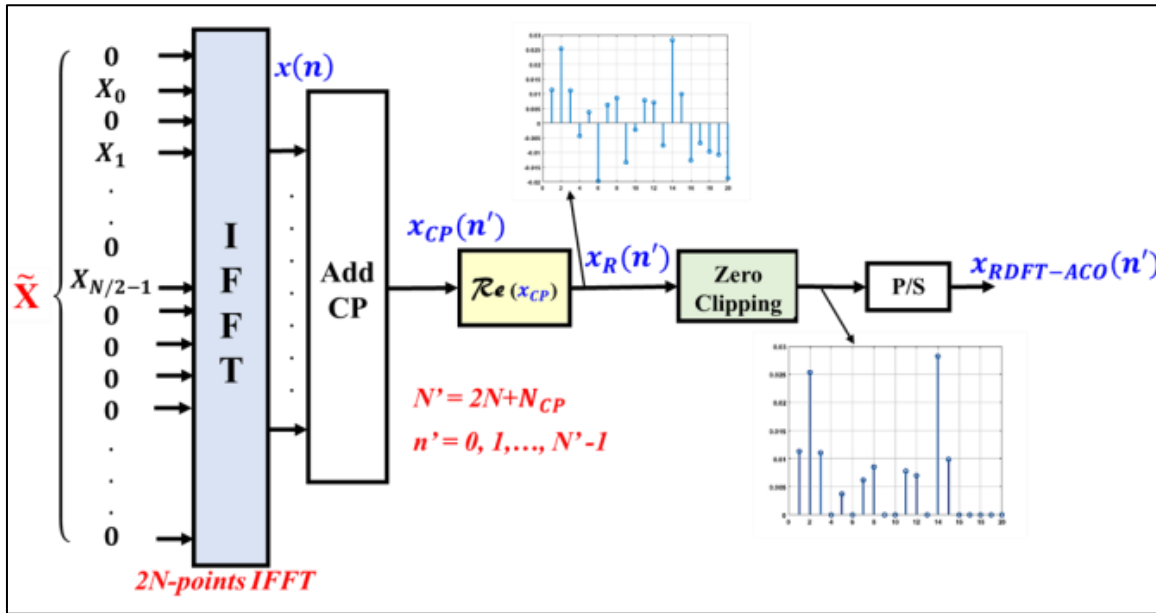
On the receiver side, after perfect synchronization of the signal, the CP is removed, and the FFT block is applied (as shown in Figure 3-b). The resulting output, assuming back-to-back transmission [21] should be as given in equation (7):

$$Y(n) = \begin{cases} 0 & \text{for } n = 0, \\ X(n-1); & \text{for } n \in \{1, 2, \dots, N\}, \dots\dots\dots(7) \\ X^*(N-1-n); & \text{for } n \in \{\frac{N}{2}+1, \dots, 2N-1\}. \end{cases}$$

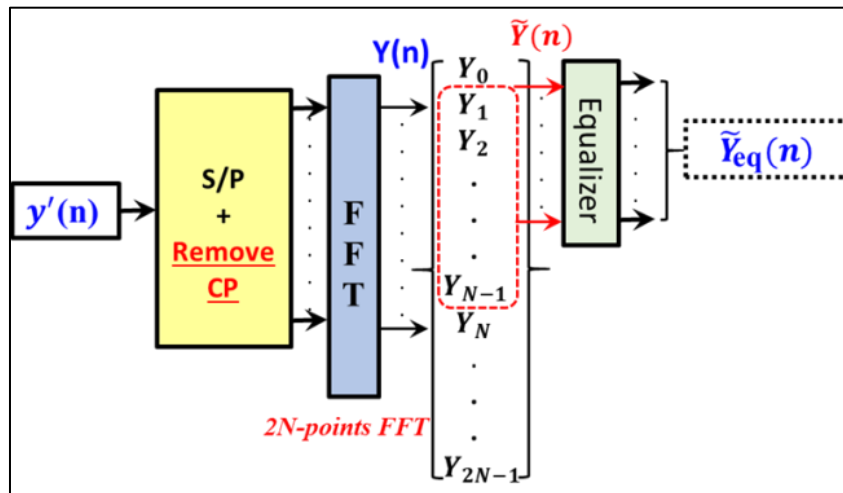
The useful odd subcarriers are retrieved after equalizing $\tilde{Y}(n)$ from equation (8), as shown in Figure 3-b.

$$\tilde{Y}(n) = Y(n + 1), \quad n = 0, 1, \dots, N - 1 \dots\dots\dots(8)$$

Thus, the equalized signal $\tilde{Y}_{eq}(n)$ is QAM de-mapped, and the transmitted bits are recovered.



(a)



(b)

Figure 3 Block diagram of a Real-DFT ACO-OFDM: (a) Modulator, (b) Demodulator

2.4. Proposed Low-Complexity Improved ACO-OFDM schemes

In the ACO-OFDM schemes described earlier, the transmitted bits modulate only the odd subcarriers, which are then retrieved from the odd subcarriers on the receiver side.

An efficient method of ACO-OFDM is Diversity-Combined ACO-OFDM (DC-ACO-OFDM) [11]. This approach operates on the received signal without modifying the transmitter, as in conventional ACO-OFDM. At the receiver, both odd and even subcarriers are used after equalization. It is important to note that, for the Real-DFT-based DC-ACO-OFDM, equalization is performed directly on the FFT output $Y(n)$, as shown in Fig. 3-b. The equalized signal is divided into odd and even parts Y_{even} and Y_{odd} , with each part being input into an IFFT or IDHT to generate the odd and even signals in the time domain. Then, the corresponding odd time-domain signal y_{odd} is used to estimate the potential DC-offset denoted as $Y(0)$, which is crucial for accurate demodulation and signal reconstruction (9).

$$Y(0) = \sum_{n=0}^{2N-1} |y_{odd}(n)| \dots\dots\dots(8)$$

Figure 4 shows the detailed steps of this process, for respectively, both the DHT-based and proposed Real-DFT-based DC-ACO-OFDM demodulators. Through a non-linear combining process, another IDHT or IFFT is applied to reconstruct the bipolar signal of the even part, denoted as y'_{even} . To do that, the even component, with the zeroth subcarrier replaced by $Y(0)$, is used to produce the output signal y_{even} . The absolute value of y_{even} is then multiplied by the sign of y_{odd} to reconstruct y'_{even} . The combined signal y' is then obtained using (10), where α is a weighting factor.

$$y' = (1 - \alpha)y_{odd} + \alpha y'_{even} \dots \dots \dots (9)$$

Finally, a DHT block, respectively (an FFT block for Real-DFT scheme) is performed on signal y' for de-mapping and data recovery (Cf. Figure 4). More details about Diversity-Combining and Improved Noise Cancellation techniques can be found in [11]- [17].

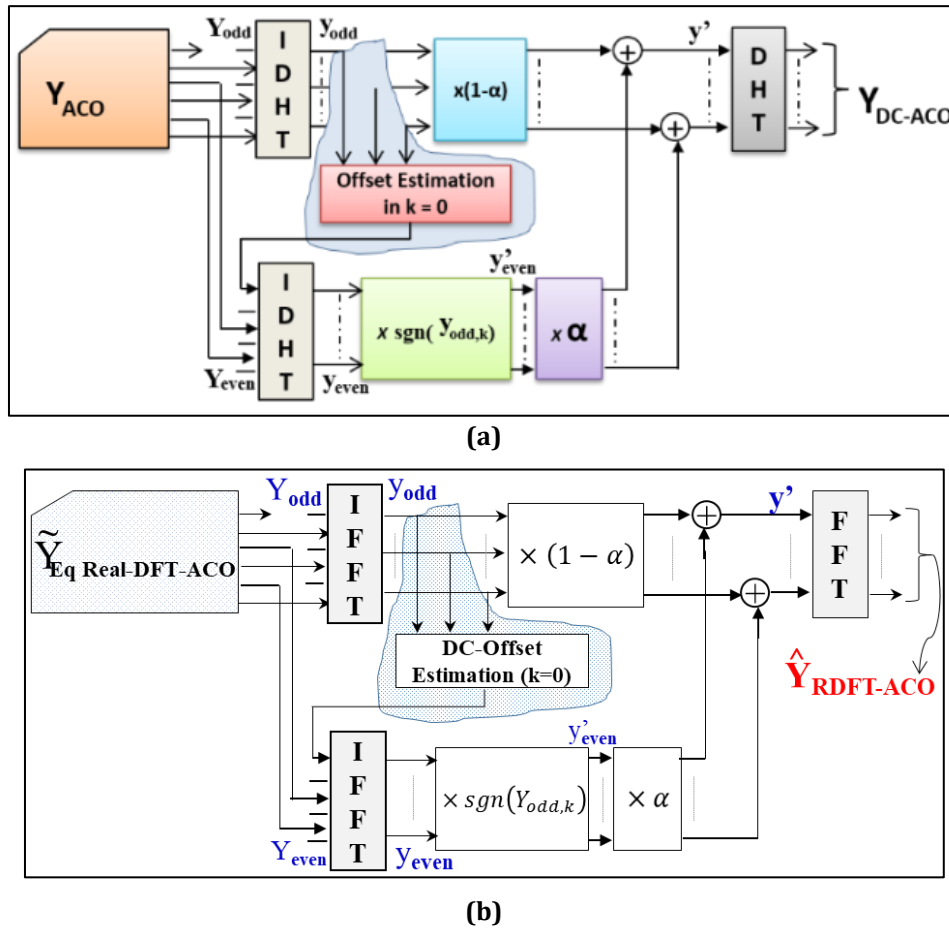


Figure 4 Block diagram of the: (a) DHT-based DC-ACO-OFDM, (b) Real-DFT-based DC-ACO-OFDM

Given the relatively high computational complexity of Diversity-Combining technique, practical issues such as increased hardware costs and higher energy consumption may arise. To address these concerns, the Improved Noise Cancellation (INC) technique is proposed in this paper as best alternative. It incorporates the DC-Offset estimation using a Virtual Clean Windows (VCW) concept. Due to clipping at the transmitter, the ACO-OFDM signal contains many zeros. On the receiver side, these zeros create a virtual "clean" window that allows for the observation of degradation and noise without interference from the data signal. Figure 5 presents the block diagram of the DHT-based and Real-DFT-based INC-ACO-OFDM after the equalization step in their respective DHT-based or Real-DFT-based ACO-OFDM schemes. As shown, the equalized symbols in each case are fed into an IDHT or IFFT block, which generates the time-domain signal y_{ACO} , as expressed in equation (11). The signal y_{ACO} represents $y_{DHT-ACO}$ in the DHT-based scheme and y_{RACO} in the Real-DFT-based scheme.

$$y_{ACO}(n) = x_{ACO}(n) + d + w_1(n) \dots \dots \dots (11)$$

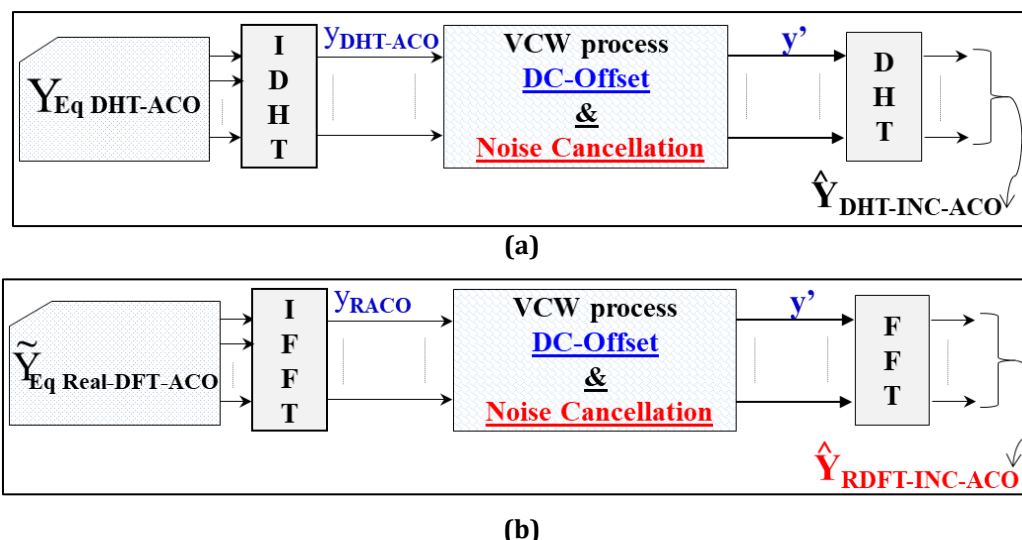


Figure 5 Block diagram of the: (a) DHT INC-ACO-OFDM demodulation and (b) Real-DFT-based INC-ACO-OFDM

The variable x_{ACO} represents the transmitted ACO-OFDM signal through the channel. d and w_1 correspond to the DC-offset and the noise of the received signal, respectively. Based on the antisymmetric property (2) and the zero-clipping operation, the identification of the VCW can be simplified to a series of paired detections between two (02) hypotheses [16] as described in equations (12) and (13):

$$H_0 : \begin{cases} y_{ACO}(n) > 0 \\ y_{ACO}(n + N) = 0 \end{cases} \quad n = 0, 1, \dots, N - 1 \dots\dots\dots(12)$$

$$H_1 : \begin{cases} y_{ACO}(n) = 0 \\ y_{ACO}(n + N) > 0 \end{cases} \quad n = 0, 1, \dots, N - 1 \dots\dots\dots(13)$$

Using the established hypotheses H0 and H1, the decision criterion is defined by equation (14):

$$y_{ACO}(n) - d \underset{H_1}{\overset{H_0}{\geq}} y_{ACO}(n + N) - d \dots\dots\dots(14)$$

Therefore, based on equation (14), the VCW can be represented as a set of indices: $I \triangleq \{n_i, i = 0, 1, \dots, N - 1\}$ where equation (15) is given by:

$$n_i = \begin{cases} i + N & \text{if } H_0 \text{ is true} \\ i & \text{if } H_1 \text{ is true} \end{cases} \dots\dots\dots(15)$$

Once the positions in I are identified through the VCW process, the DC-offset, denoted a DC_{Off} , can be estimated using equation (16), where $e(k)$ represents the estimation error and its power, is as large as $1/N^2$ of the $w_1(k)$ power:

$$DC_{Off} = \frac{1}{N} \sum_{i=0}^{N-1} y_{ACO}(n_i) = d + e(k) \dots\dots\dots(16)$$

For a sufficiently large N, the estimation error $e(k)$ becomes negligible, allowing d to closely approximate the true DC-offset. Once the DC-offset value is determined, it can be removed from the noise in $y_{ACO}(n)$ using equations (17)-(18):

$$y_1(n) = \begin{cases} y_{ACO}(n) - DC_{Off} & \text{if } n \in \bar{I} \\ 0 & \text{if } n \in I \end{cases} \dots\dots\dots(16)$$

$$y_2(n) = \begin{cases} y_1(n) & \text{if } y_1(n) \geq 0 \\ 0 & \text{if } y_1(n) < 0 \end{cases} \dots\dots\dots(16)$$

Thus, data can be simply recovered by extracting symbols from the odd subcarriers of $y_2(k)$.

Computational complexity is defined as the number of arithmetic multiplications and additions (operations) required in the transmitter and receiver blocks. For an IFFT/FFT or IDHT/DHT block size of N, the complexity is approximately

$O(5N \times \log_2(N))$ operations [21]. The INC approach reduces the computational complexity of the Diversity-Combining technique by eliminating the need for one IDHT or IFFT block. To evaluate the complexity requirements of the proposed ACO-OFDM schemes, Table 1 provides a comparison of their respective computational complexity. The following section presents the methodology of the study.

Table 1 Comparative Computational complexity of the studied ACO-OFDM schemes

N°	OFDM Schemes	Number of IFFT/FFT or IDHT/DHT blocks	Total Computational Complexity in terms of Big-O Notation
1	ACO-OFDM	IFFT in Tx 1FFT in Rx	$10N_{IFFT} \times \log_2(N_{IFFT})$
2	DHT-ACO-OFDM ^[a]	1DHT in Tx 1DHT in Rx	$O(10N_{IFFT} \times \log_2(N_{IFFT}))$
3	Real-DFT-ACO-OFDM	1IFFT in Tx 1FFT in Rx	$\frac{5N_{IFFT}}{2} \times \log_2\left(\frac{N_{IFFT}}{2}\right) + 5N_{IFFT} \times \log_2(N_{IFFT})$
4	Conv. DC-ACO-OFDM	1IFFT in Tx 2FFT+2IFFT in Rx	$25N_{IFFT} \times \log_2(N_{IFFT})$
5	Conv. INC-ACO-OFDM	1IFFT in Tx 2FFT+1IFFT in Rx	$20N_{IFFT} \times \log_2(N_{IFFT})$
6	DHT INC-ACO-OFDM ^[a]	1 IDHT in Tx 2 DHT+ 1 IDHT in Rx	$20N_{IFFT} \times \log_2(N_{IFFT})$
7	Real-DFT INC-ACO-OFDM	1IFFT in Tx 2FFT+1IFFT in Rx	$\frac{5N_{IFFT}}{2} \times \log_2\left(\frac{N_{IFFT}}{2}\right) + 15N_{IFFT} \times \log_2(N_{IFFT})$

^[a] With computational saved and simpler system [16],[17]

2.5. Methodology and Simulation

Simulations are conducted in an AWGN channel with MATLAB R2021a. Each OFDM scheme is generated with an IDHT/DHT or IFFT/FFT size of $N=512$. The DHT-based scheme employs 2~16-PAM mapping, while the conventional and Real-DFT schemes use 4~256-QAM. A cyclic prefix (CP) of 16 samples is applied. BER performance is evaluated through Monte Carlo simulations.

Various performance metrics are used in the literature to compare modulation schemes in optical systems. One common metric is the optical signal-to-noise ratio (SNR), which quantifies performance based on the ratio of optical power to the standard deviation of zero-mean noise power. Another widely used metric is the electrical energy-per-bit to single-sided noise power spectral density ratio $E_{b(\text{elec})}/N_0$. Additionally, the effective SNR, defined as the ratio of OFDM signal power to effective noise power, serves as a key performance comparison. Notably, as $E_{b(\text{elec})}/N_0$ increases, the SNR also improves. In this study, we consider $E_{b(\text{elec})}/N_0$ to analyze the BER performances of the investigated ACO-OFDM schemes in an AWGN channel.

First, a BER performance comparison is conducted between conventional ACO-OFDM and Real-DFT-based ACO-OFDM. A similar analysis is then performed for conventional ACO-OFDM and the corresponding DHT-based scheme. Next, the performance of both the Diversity-Combining and Improved Noise Cancellation approaches is compared to that of its improved conventional ACO-OFDM. Finally, computational complexity of the proposed improved ACO-OFDM is discussed and compared with the conventional INC-ACO-OFDM technique [30]. INC-ACO-OFDM is chosen as the

reference for comparison due to its lower complexity compared to DC-ACO-OFDM, aligning with our objective of developing a computationally efficient and enhanced variant of ACO-OFDM.

To simplify the notation of the modulation techniques in this paper, we will refer to the Real-DFT-based ACO-OFDM technique as “RDFT ACO” and the conventional ACO-OFDM technique as “Conv ACO”. Similarly, the DHT-based ACO-OFDM, DHT-based INC-ACO-OFDM, and DHT-based DC-ACO-OFDM will be denoted as “DHT ACO”, “DHT INC-ACO”, and “DHT DC-ACO”, respectively. The same notation applies to Real-DFT-based INC-ACO-OFDM, Real-DFT-based DC-ACO-OFDM, and conventional DC-ACO-OFDM, which will be referred to as “RDFT INC-ACO”, “RDFT DC-ACO”, and “Conv DC-ACO”, respectively.

3. Results and discussion

In this section, we present the results obtained according to the previously methodology. A comparison between RDFT ACO-OFDM and conventional ACO-OFDM techniques is presented in Figure 6. The results show that RDFT ACO-OFDM achieves a similar BER performance to conventional ACO-OFDM, regardless of the QAM constellation. This indicates that the RDFT method does not affect system performance as shown in [20]-[21], because it serves merely as an alternative approach to bypass the use of Hermitian symmetry, which is typically employed in conventional ACO-OFDM.

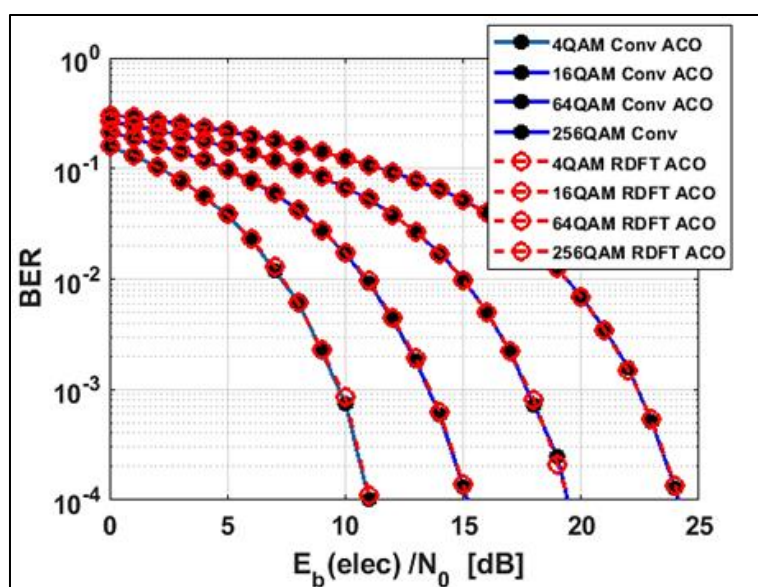


Figure 6 BER performance of RDFT ACO-OFDM vs Conventional ACO-OFDM as a function of $E_{b(\text{elec})}/N_0$

Moreover, for a fixed $E_{b(\text{elec})}/N_0$, we observe that the BER deteriorates as the constellation size increases. This can be explained by the Shannon's Second Theorem, where to transmit more bits (for example, moving from 4QAM to 16-QAM or more), a sufficiently high $E_{b(\text{elec})}/N_0$ is required to ensure the same BER.

Figure 7 presents a BER comparative study between conventional ACO-OFDM and DHT ACO-OFDM techniques in terms of $E_{b(\text{elec})}/N_0$. As shown in Figure 6, the BER improves with SNR increasing in Figure 7.

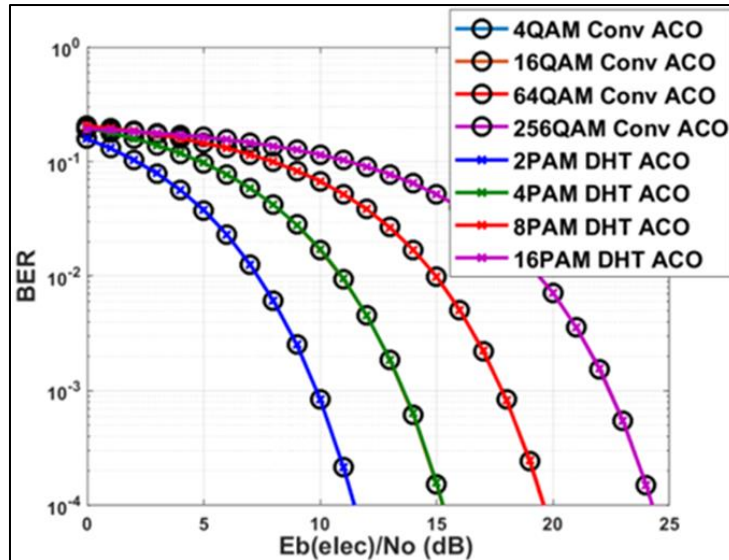


Figure 7 BER performance of DHT ACO-OFDM vs conventional ACO-OFDM as a function of $E_{b(elec)}/N_0$

This can be attributed to the fact that higher SNR reduces the impact of channel noise on the transmitted signal, leading to more accurate symbol transmission. For any M-PAM constellation, the DHT-ACO technique demonstrates a BER performance similar to both M^2 -QAM RDFT ACO-OFDM and conventional M^2 -QAM ACO-OFDM modulation. This can be explained by the fact that the spectral efficiency of an M-PAM constellation matches that of an M^2 -QAM constellation with Hermitian symmetry in conventional ACO-OFDM. Since both constellations transmit the same number of bits per symbol, it follows that the M-PAM and M^2 -QAM symbols are subjected to a similar level of noise impact. Since the DHT and IDHT use the same kernel, employing identical circuitry in both the transmitter and receiver simplifies the design and reduces power consumption [16].

Figure 8 compares the BER performance achieved by simulating Diversity-Combining and Improved Noise Cancellation in the DHT ACO-OFDM scheme, as a function of $E_{b(elec)}/N_0$ for different M-PAM formats.

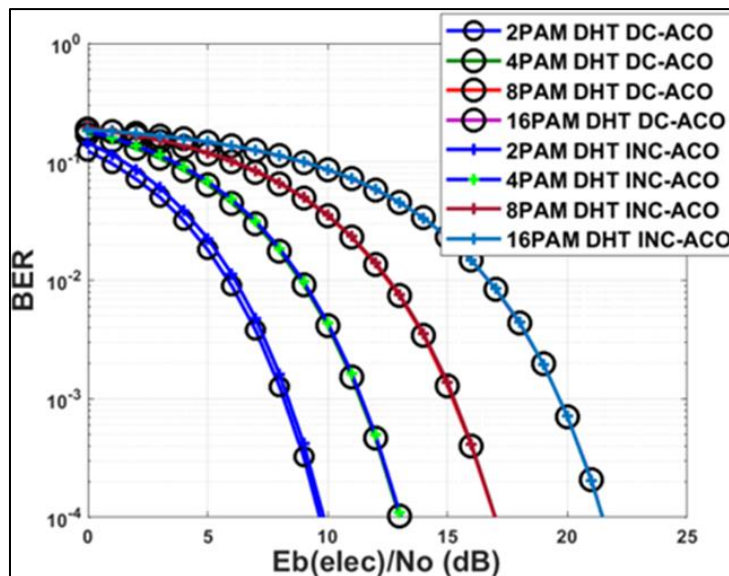


Figure 8 BER performance of DHT INC-ACO vs DHT DC-ACO as a function of $E_{b(elec)}/N_0$

It can be seen that both techniques provide similar BER performance, with an approximate 3 dB SNR gain compared to conventional, RDFT-based, or DHT-based ACO-OFDM (see Figure 8 versus Figure 6 and Figure 7). This improvement is

attributed to the effective demodulation offered by both Diversity-Combining and Improved Noise Cancellation, which reduce the system's noise impact by about half.

Similar BER performance are observed in both Figure 9 and Figure 10 when simulating the Diversity-Combining or Improved Noise Cancellation approaches in RDFT-based ACO-OFDM, compared to their corresponding Conventional Diversity-Combined ACO-OFDM.

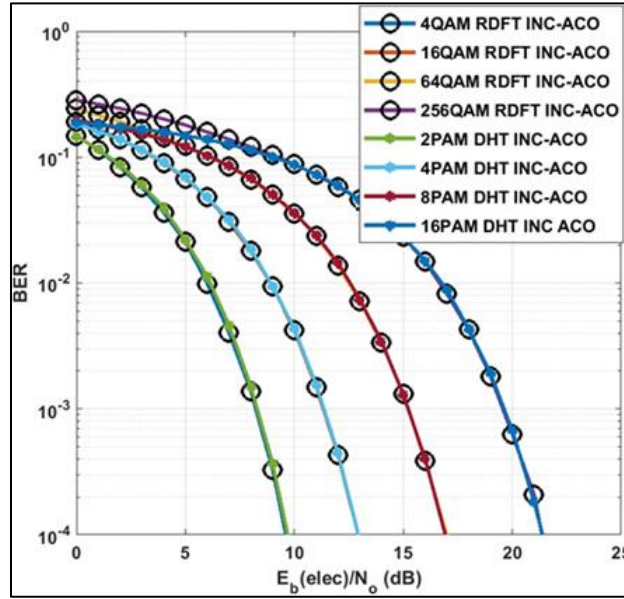


Figure 9 BER performance of RDFT INC-ACO vs DHT INC-ACO as a function of $E_{b(elec)}/N_0$

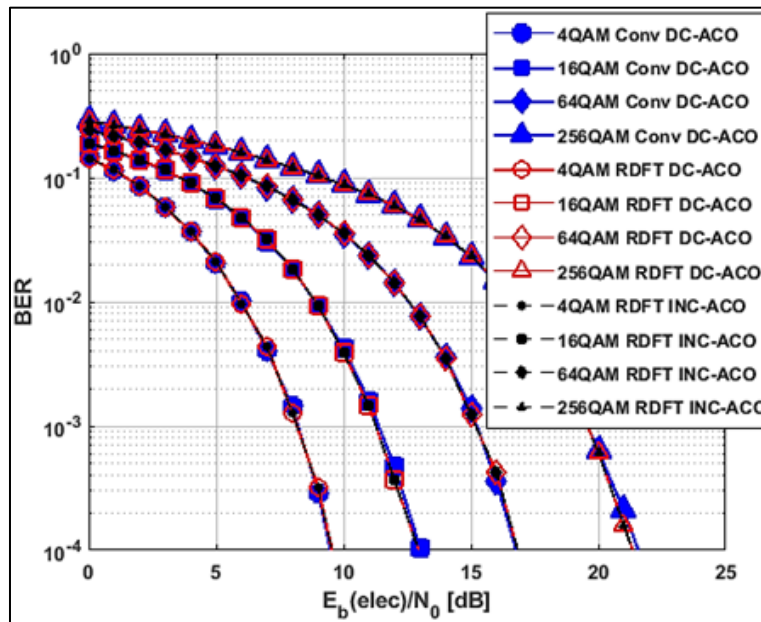


Figure 10 BER performance of RDFT DC-ACO and RDFT INC-ACO vs DC-ACO-OFDM as a function of $E_{b(elec)}/N_0$

This demonstrates again the performance enhancement that can be introduced by these proposed alternatives for ACO-OFDM, as also shown in [1098].

Furthermore, as Conventional ACO-OFDM uses complex-valued FFT and IFFT, which are computationally more expensive due to complex arithmetic operations, it has higher constant factors than Real-DFT method, but both have the same Big-O complexity. The complexity of Real-DFT method generally comes with higher constant factors than DHT, because Real-DFT involves some additional processing compared to DHT. So, while Real-DFT-based ACO-OFDM and

Conventional ACO-OFDM have the same Big-O complexity, DHT-based ACO-OFDM is the more efficient one in practice, with lower constant factors and simpler computations. Based on the results and computational complexity presented in Table 1, we demonstrate that the Improved Noise Cancellation technique in both DHT-based and Real-DFT-based ACO-OFDM enables low-complexity, enhanced ACO-OFDM demodulation schemes.

4. Conclusion

The DHT-based and Real-DFT INC-ACO-OFDM systems presented in this paper offer a highly innovative and promising solution. Optical systems using IM/DD would benefit significantly from this approach in practical applications. The proposed schemes, analyzed in an AWGN channel, demonstrate a 3 dB power gain compared to conventional ACO-OFDM. For low-complexity yet high-performance optical network systems, the DHT-based and Real-DFT INC-ACO-OFDM schemes stand out as strong candidates, with a preference for DHT-based solutions due to their lower computational complexity. This study merits further research under realistic conditions, such as optical fiber transmission or Light-Fidelity communications, with considerations for multi-layer aspects and error correction.

Compliance with ethical standards

Acknowledgments

We thank the Centre Autonome de Perfectionnement (CAP) of EPAC/University of Abomey-Calavi and the University of UNSTIM, Abomey, for their initiative in the research strategy and for fostering collaboration through student exchanges and thesis supervision.

Disclosure of conflict of interest

No conflict of interest to be disclosed.

References

- [1] Anass, K., Hamza, O., Zhou, M., Younes, Z. Performance analysis of a multi-user outdoor visible light communication system using wavelength division multiplexing (WDM) with RZ-OOK and NRZ-OOK modulations for V2X communications. *e-Prime - Advances in Electrical Engineering, Electronics and Energy*. 2025; 11(100900). ISSN 2772-6711. <https://doi.org/10.1016/j.prime.2025.100900>.
- [2] Hujijo, H. S. R. and Ilyas, M. Enhancing spectral efficiency with low complexity filtered-orthogonal frequency division multiplexing in visible light communication system, *ETRI Journal*. 2024; 46:1007–1019, DOI 10.4218/etrij.2023-0300.
- [3] Lowery, A. J., & Armstrong, J. Orthogonal frequency division multiplexing for dispersion compensation of long-haul optical systems. *Opt. Express* 14. 2006; 2079-2084.
- [4] Dai, L., Liu, Z., Meng, S. and Zhao, Y. Research on the Pulse-position Modulation in the Digital Communication System," *International Conference on Wireless Communications and Smart Grid (ICWCSG)*, Hangzhou, China. 2021; 8-12, doi: 10.1109/ICWCSG53609.2021.00009.
- [5] Nanjun, Y., Pengzhao, W., and Zhiyi, Z. Design of Digital Pulse-Position Modulation System. *Journal of Physics: Conference Series*. 2021; 2093(012030), doi: 10.1088/1742-6596/2093/1/012030.
- [6] Zhang, Y. Design of a pulse amplitude modulation-based communication system. *Highlights in Science, Engineering and Technology*. 2023; 53: 123-132. <https://doi.org/10.54097/hset.v53i.9695>.
- [7] Farid, S., Saleh, M., Elbadawy, H., & Elramly, S. Novel Unipolar Optical Modulation Techniques for Enhancing Visible Light Communication Systems Performance. *IEEE Access*. 2022; 10: 1-1. <https://doi.org/10.1109/ACCESS.2022.3186007>.
- [8] Xu, X.-Y., Zhang, Q., & Yue, D.-W. Discrete Hartley transform-based dual-mode index modulation OFDM for visible light communications. *Applied Optics*, 2023 ; 62(31): 8442-8450. <https://doi.org/10.1364/AO.504221>.
- [9] Selvi, M., Thirunambi, V., Sriram, R. and Srinivasan, E. FPGA-based OFDM Systems for 5G and High-Speed Communication: A Comprehensive Review," *2024 8th International Conference on Electronics, Communication and Aerospace Technology (ICECA)*, Coimbatore, India, 2024, pp. 232-237, doi: 10.1109/ICECA63461.2024.10800844.

- [10] Miah, M. S., Khan, M., Niu, M. -b., and Armada, A. G. Comparative Performance Analysis of Peak to Average Power Ratio in OFDM, SLM and PTS Systems. 9th International Conference on Computer and Communication Systems (ICCCS), Xi'an, China. 2024; 712-717, doi: 10.1109/ICCCS61882.2024.10602891.
- [11] Al-Gharabally, M., and Almutairi, A. F. Frequency-domain subcarrier diversity receiver for discrete Hartley transform OFDM systems. *J Wireless Com Network*. 2019; 78. doi:10.1186/s13638-019-1398-0.
- [12] Çürük, S., M. Comparison of Fourier and Trigonometric Transform based Multicarrier Modulations for Visible Light Communication. *TJST*. 2024 Sept; 19(2):397-405. doi:10.55525/tjst.1452146.
- [13] Wu, M., Xie, Y., Shi, Y., Zhang, J., Yao, T., & Liu, W. An Adaptively Biased OFDM Based on Hartley Transform for Visible Light Communication Systems. *IEICE Transactions on Fundamentals of Electronics, Communications and Computer Sciences*. 2024; E107.A(6): 928-931. <https://doi.org/10.1587/transfun.2023EAL2059>.
- [14] Lu, C.F., et al. Study of LACO-OFDM low complexity reception method based on discrete Hartley transform. *Optical Communication Technology*. 2023; 47(02): 48-52.
- [15] Moreolo, S. M., Munoz, R., and Junyent, G. Novel Power Efficient Optical OFDM Based on Hartley Transform for Intensity-Modulated Direct-Detection Systems. *Journal of Lightwave Technology*. 2010; 28(5): 798-805. doi: 10.1109/JLT.2010.2040580.
- [16] Fréjus Owolabi, S. M., Zola Cédric Bosco, A., Merci-Ange, M. F., Patrick, S., Michel, D. and Christelle, A. -B. Performance Analysis of Improved Noise Cancellation Discrete Hartley Transform ACO-OFDM in a AWGN channel. *International Conference on Cyber-Enabled Distributed Computing and Knowledge Discovery (CyberC)*, Guangzhou, China. 2024; 121-126, doi: 10.1109/CyberC62439.2024.00030.
- [17] Miriyala, G., Mallaiah, R., Sathyaprasad, A. K., Vejandla, K. and Vakamulla, V. M. A Low-Complex and Power-Efficient Optical OFDM for VLC Systems. *Journal of Lightwave Technology*. 2024 Dec; 1-9. doi: 10.1109/JLT.2024.3521952.
- [18] Hujijo, H. S. R., Ilyas, M. A. Novel Flip-Filtered Orthogonal Frequency Division Multiplexing-Based Visible Light Communication System: Peak-to-Average-Power Ratio Assessment and System Performance Improvement. *Photonics*. 2025; 12(1):69. <https://doi.org/10.3390/photonics12010069>.
- [19] Bai, R., Hranilovic, S., and Wang, Z. Low-Complexity Layered ACO-OFDM for Power-Efficient Visible Light Communications. *IEEE Transactions on Green Communications and Networking*. 2022; 6(3): 1780-1792. doi: 10.1109/TGCN.2022.3147970.
- [20] Gallo, R., Abdelaziz, A., Alghoniemy, M., & Shalaby, H. Real-DFT Based DCO-OFDM and ACO-OFDM for Optical Communications Systems. *International Conference on Transparent Optical Networks (ICTON)*. 2019; 1-4. <https://doi.org/10.1109/ICTON.2019.8840573>.
- [21] Hasan, J., Khalighi, M.-A., Jungnickel, V., Alves, L., and Béchadergue, B. An Energy-Efficient Optical Wireless OFDMA Scheme for Medical Body-Area Networks. *IEEE Transactions on Green Communications and Networking*. 2022; 6(1): 1. <https://doi.org/10.1109/TGCN.2022.3161413>.
- [22] Hu, W. -W., Chang, C., Lin, X. PAPR Reduction Techniques in ADO-OFDM for VLC Systems. 10th International Conference on Applied System Innovation (ICASI), Kyoto, Japan. 2024; 29-30. doi: 10.1109/ICASI60819.2024.10547967.
- [23] Zenhom, Y. A., Hamad, E. K. I., Alghassab, M., Elnabawy, M. M. Optical-OFDM VLC System: Peak-to-Average Power Ratio Enhancement and Performance Evaluation. *Sensors (Basel)*. 2024; 24(10):2965. doi: 10.3390/s24102965.
- [24] Schulze, H., and Hoeher, P.A. Asymmetrically Clipped Optical Hadamard Coded Modulation (ACO-HCM). *IEEE Photonics J*. 2023; 15:3237959. doi: 10.1109/JPHOT.2023.3237959.
- [25] Sharan, N., and Ghorai, S. K. Hybrid Scheme of Precoder with μ -Law Componder for PAPR Reduction and Nonlinearity Improvement in ADO-OFDM System. *Int. J. Commun. Syst*. 2021; 34:e4961. doi: 10.1002/dac.4961.
- [26] Baig, M. S., Alresheedi M. T., Mahdi, M. A., and Abas, A. F. A Spectrally Efficient Modified Asymmetrically and Symmetrically Clipped Optical (MASCO)-OFDM for IM/DD Systems. *Opt. Quantum Electron*. 2023; 55:411. doi: 10.1007/s11082-023-04611-4.
- [27] Zhang, T., Sun, L., Zhao, C., Qiao, S., and Ghassemlooy, Z. Low complexity receiver for HACO-OFDM in optical wireless communications. *IEEE Wireless Commun. Lett*. 2021; 10(3):572-575.

- [28] Geng, Z., Tang, X., and Dong, Y. Layered Optical OFDM Schemes for IM/DD OWC Systems. IEEE Wireless Communications and Networking Conference (WCNC), Dubai, United Arab Emirates. 2024; 01-06. doi: 10.1109/WCNC57260.2024.10571016.
- [29] Liu, X., Zhou, J., and Zhang, W. Information Theoretic Limits of Improved ACO-OFDM Receivers in Optical Intensity Channels With Time Dispersion. IEEE Open Journal of the Communications Society. 2024; 5:489-502. doi: 10.1109/OJCOMS.2023.3347733.
- [30] Aupetit-Berthelemot, C., and Sanya, M. F. O. An IFFT/FFT size efficient improved ACO-OFDM scheme for next-generation passive optical network. 21st European Conference on Networks and Optical Communications (NOC), Lisbon, Portugal. 2016; 111-116, doi: 10.1109/NOC.2016.7506995.